Peroxisome proliferator–activated receptor γ ligands inhibit development of atherosclerosis in LDL receptor–deficient mice

Andrew C. Li,[1] Kathleen K. Brown,[2] Mercedes J. Silvestre,[3]
Timothy M. Willson,[4] Wulf Palinski,[3] and Christopher K. Glass[1,3]

[1]Department of Cellular and Molecular Medicine, University of California, San Diego, La Jolla, California, USA
[2]Department of Metabolic Diseases, Glaxo Wellcome Research and Development, Research Triangle Park,
 North Carolina, USA
[3]Department of Medicine, University of California, San Diego, La Jolla, California, USA
[4]Department of Medicinal Chemistry, Glaxo Wellcome Research and Development, Research Triangle Park, North Carolina, USA

Address correspondence to: Andrew C. Li, Department of Cellular and Molecular Medicine,
University of California, San Diego, 9500 Gilman Drive, La Jolla, California 92093-0651, USA.
Phone: (858) 534-7559; Fax: (858) 534-8549; E-mail: acli@ucsd.edu.

The Palinski and Glass laboratories contributed equally to this work.

Received for publication May 18, 2000, and accepted in revised form July 5, 2000.

The peroxisome proliferator–activated receptor γ (PPARγ) is a nuclear receptor that regulates fat-cell development and glucose homeostasis and is the molecular target of a class of insulin-sensitizing agents used for the management of type 2 diabetes mellitus. PPARγ is highly expressed in macrophage foam cells of atherosclerotic lesions and has been demonstrated in cultured macrophages to both positively and negatively regulate genes implicated in the development of atherosclerosis. We report here that the PPARγ-specific agonists rosiglitazone and GW7845 strongly inhibited the development of atherosclerosis in LDL receptor–deficient male mice, despite increased expression of the CD36 scavenger receptor in the arterial wall. The antiatherogenic effect in male mice was correlated with improved insulin sensitivity and decreased tissue expression of TNF-α and gelatinase B, indicating both systemic and local actions of PPARγ. These findings suggest that PPARγ agonists may exert antiatherogenic effects in diabetic patients and provide impetus for efforts to develop PPARγ ligands that separate proatherogenic activities from antidiabetic and antiatherogenic activities.

J. Clin. Invest. **106**:523–531 (2000).

Introduction

Complications of atherosclerosis are the leading cause of death in Western societies and have an extremely high incidence in individuals with type 2 diabetes mellitus (1, 2). Atherosclerosis is initiated by the accumulation of plasma LDL in the arterial wall, its oxidation, and the recruitment of circulating monocytes (3, 4). Once monocytes in the arterial intima have undergone phenotypic transformation to macrophages, they take up oxidized LDL (oxLDL) via several scavenger receptors that include scavenger receptor A (SR-A), CD36, and macrosialin (5–7). This results in massive cholesterol accumulation and formation of foam cells. Interactions between oxLDL, macrophages, smooth muscle cells infiltrated from the arterial media, and T cells recruited from the circulation result in a chronic inflammatory condition that is thought to influence the further evolution of early atherosclerotic lesions toward more advanced, clinically relevant lesions (8). Interactions between arterial cells are mediated by an array of cytokines and adhesion molecules (9), and increasing experimental evidence suggests that many of these factors promote atherogenesis. For example, hypercholesterolemic mice in which the gene encoding macrophage chemotactic protein 1 (MCP-1) has been disrupted are resistant to the development of atherosclerosis (10, 11). In analogy, disruption of the *SR-A* and *CD36* genes results in a significant reduction of hypercholesterolemia-induced atherosclerosis in mice (12, 13). These observations suggest that interventions directed at altering the genetic responses of vascular cells to proatherogenic stimuli, such as hypercholesterolemia, may be beneficial.

Several regulatory pathways have been identified that control the expression of potentially atherogenic genes. These include NF-κB, a transcription factor involved in the regulation of many proinflammatory factors and adhesion molecules, such as TNF-α and gelatinase B (14, 15). Recent studies have also documented the expression of the peroxisome proliferator–activated receptor γ (PPARγ) in macrophage foam cells, endothelial cells, and smooth muscle cells of human and murine atherosclerotic lesions (16–20). PPARγ is a member of the nuclear receptor superfamily of ligand-dependent transcription factors that both positively and negatively regulate gene expression in response to the binding of a number of fatty acid metabolites, including oxidized linoleic acid (9- and 13-HODE) and

15 deoxy $\Delta^{2,14}$ prostaglandin J_2 (21–23). PPARγ is expressed in many other tissues and is particularly highly expressed in fat. PPARγ promotes adipocyte differentiation in vitro and has recently been shown to be essential for the development of adipose tissue in vivo (24–26). PPARγ also appears to play a critical role in glucose homeostasis, because it is the molecular target of a class of insulin-sensitizing drugs referred to as thiazolidinediones (TZDs) (27).

The biological roles of PPARγ in the macrophage and its effects on atherosclerosis are uncertain. PPARγ-specific ligands have been shown to inhibit the expression of a number of proinflammatory genes, including *TNF-α*, *IL-1β*, *iNOS*, and *gelatinase B* (28, 29). These findings suggested that PPARγ functions as a negative regulator of macrophage activation and that synthetic PPARγ ligands might exert anti-inflammatory and antiatherogenic effects. Consistent with this, PPARγ ligands have recently been shown to inhibit inflammatory bowel disease in a rodent model (30). However, PPARγ has also been shown to stimulate transcription of the *CD36* gene (19, 21). In conjunction with the finding that PPARγ can be activated by 9- and 13-HODE present in oxLDL, a "PPARγ cycle" has been proposed in which oxLDL lipids would induce the activity of PPARγ, leading to increased expression of CD36, which in turn would increase the uptake of oxLDL. This cycle would thus promote foam-cell formation and atherosclerosis.

Resolving the question of whether PPARγ agonists promote or inhibit atherosclerosis is of clinical importance because many patients with type 2 diabetes, who are at high risk of developing atherosclerosis and its complications, are currently using PPARγ agonists for the control of hyperglycemia. To determine whether the activation of PPARγ promotes or inhibits the development of atherosclerosis in an animal model, we administered two structurally distinct PPARγ-specific ligands to LDL receptor-deficient (LDLR$^{-/-}$) mice fed a Western-style diet and measured their effects on lipid and glucose metabolism, extent of atherosclerosis, and expression of potential target genes in the artery wall. Both PPARγ-specific ligands exerted potent antiatherogenic effects in male mice despite upregulation of CD36 mRNA. Antiatherogenic effects correlated with improved insulin sensitivity and inhibition of TNF-α and gelatinase B expression.

Methods

Animals and diet. A breeding colony was generated from the tenth-generation homozygous LDLR$^{-/-}$ mice in a C57BL/6 background (The Jackson Laboratories, Bar Harbor, Maine, USA). In three separate experiments, three groups of both males and females were matched for age (8 to 12 weeks), plasma cholesterol, and glucose levels before feeding. Four animals were housed per cage and in a facility with an 11-hour light cycle (light, 7 am to 6 pm). All three groups were fed a Western-style diet consisting of 0.01% added cholesterol and 21% milk fat (TD98338; Harlan-Teklad, Madison, Wisconsin, USA), which induced extensive atherosclerosis in the aortic origin, but not in the descending aorta at 10 weeks. In addition to the diet, one group received rosiglitazone and another group received GW7845. The animals were fed 3–4 g food/mouse/day with a drug delivery of 20 mg/kg of body weight/day. New batches of food/drug were prepared weekly and stored at 4°C. The amount of food given and the food left remaining were weighed daily. The animals were weighed every 2 weeks, and the drug dosages were adjusted accordingly. To induce extensive atherosclerosis in the aorta, in a separate experiment male mice were fed a diet containing 1.25% cholesterol and 21% milk fat (TD96121; Harlan-Teklad) for 4 months. Two weeks before sacrifice, the animals were divided into three groups. A control group received the diet treated only with the solvent, the second group received the diet together with rosiglitazone (20 mg/kg/day), and the third group received the diet and GW7845 (20 mg/kg/day). All animals had ad libitum access to water. The animal experiments were performed according to NIH guidelines and were approved by UCSD's Animal Subjects Committee.

Glucose, insulin, and lipid levels. Retro-orbital bleeds were performed before the start of the studies and every 4 weeks thereafter until the animals were sacrificed at 10 weeks. The animals were bled, nonfasted, at 10 am and blood was drawn up in EDTA-coated microcapillary tubes. Plasma was isolated from whole blood and glucose levels were determined, using a Precision QID glucometer (MediSense Inc., Bedford, Massachusetts, USA). Insulin levels were determined using a competitive radioimmunoassay (Linco Research Inc., St. Charles, Missouri, USA). Plasma cholesterol and triglyceride levels were measured by enzymatic methods using an automated bichromatic analyzer (Abbot Diagnostics, Dallas, Texas, USA). To determine the lipoprotein profiles, remaining terminal plasma samples were pooled according to the animals' respective groups, and the cholesterol content of lipoprotein fractions in plasma was determined by FPLC. One hundred milliliters of the pooled plasma was loaded onto a Superose 6B column, and 250 μL of sample fractions were collected and analyzed for cholesterol.

Oral glucose tolerance test. Two weeks before the mice were sacrificed, oral glucose tolerance tests were performed. Animals were fasted for 4 hours. Animals were gavaged with glucose (0.75 mg/g body weight) using 20% glucose. Blood samples (25 μL) were taken at 0, 15, 30, 60, and 90 minutes. Glucose levels were determined in whole blood and insulin levels in plasma.

Hemoglobin A_{1c}, nonesterified fatty acid, HDL$_c$, and drug levels. Whole blood and plasma were sent to Glaxo Wellcome Research Institute (Research Triangle Park, North Carolina, USA) for analysis for HbA$_{1c}$, HDL$_c$, and nonesterified fatty acid (NEFA) levels. The plasma was isolated immediately and quickly frozen in liquid nitrogen to prevent the breakdown of NEFA. Drug levels were determined by mass spectrometry.

Tissue preparation and morphometric analysis of atherosclerotic lesions. The heart was perfused from its apex with cold PBS treated with diethylpyrocarbonate (DEPC). The heart, containing the aortic origin, was carefully dissected. The upper half of the heart was placed in a fixative containing 4% paraformaldehyde, 5% sucrose in PBS, pH 7.4, and fixed overnight, followed by alcohol dehydration and paraffin embedding. For morphometric determination of atherosclerosis, serial 9-μm-thick sections were cut from the apex toward the base of the heart. Sections containing the aortic origin, totaling 180 μm in length, were stained with a modified van Gieson's elastin stain to enhance the contrast between the atherosclerotic intima and the surrounding tissue (31). Analysis was performed on every other section (n = 8–10 per mouse). Thus, a total length of 180 μm of the aortic origin was examined. Quantification of atherosclerosis was performed using computer-assisted image analysis, as described previously (32). All morphometry was performed by the same investigator blinded to the tissue identity.

RNA isolation from aortic valves and aortas. The upper half of the hearts, containing the aortic valves and the aortas, extending from the root to the second intercostal region and up to the carotids, were weighed and flash frozen in liquid nitrogen and stored at –80°C. Isolation of total RNA was performed using RNeasy kit (QIAGEN Inc., Valencia, California, USA) according to the manufacturer's protocol. Total RNA was treated with deoxyribonuclease I (QIAGEN Inc.) for 20 minutes at room temperature to remove contaminating genomic DNA. The amount of RNA was determined by spectrophotometry, and 200 ng of RNA was loaded onto a 1.5% agarose gel to determine its quality before analysis.

RT-PCR–based quantitative gene expression analysis. Real-time detection of PCR was performed at the Center for Aids Research Genomics Core of the Veterans Medical Research Foundation in La Jolla, California, USA. Using the Perkin-Elmer ABI Prism 7700 and Sequence Detection System software (Perkin-Elmer, Foster City, California, USA), the differential displays of mRNAs for TNF-α, MCP-1, VCAM-1, gelatinase B, macrosialin, CD36, and SR-A were determined. Briefly, 1 μg of total RNA was used to generate cDNA using an oligo dT oligodeoxynucleotide primer (T_{12-18}) following the protocol for Omniscript (QIAGEN Inc.). The following primers and probes were made: TNF-α: 5′CGGAGTC-CGGGCAGGT 3′ (forward), 5′ GCTGGGTAGAGAATG-GATGAACA 3′ (reverse), 5′ ACTTTGGAGTCATTGCTCT-GTGAAGGG AATG 3′ (probe); MCP-1: 5′ CAGCCAGATGCAGTTAACGC 3′ (forward), 5′ GCC-TACTCATTGGGATCATCTTG 3′ (reverse), 5′ CCACT-CACCTGCTGCTACTCATTCACCA 3′ (probe); VCAM-1: 5′ TGC GAGTCACCATTGTTCTCAT 3′ (forward), 5′ CATGGTCAGAACGGACTTGGA 3′ (reverse), 5′ ACCCA-GATAGACAGCCCACTAAACGCGAA 3′ (probe); gelatinase B: 5′ TCACCTTCACCCGCGTGTA 3′ (forward), 5′ GTGCTCCGCGACACCAA 3′ (reverse), 5′ ACCCGAAGCG-

GACATTGTCATCCAG 3′ (probe); macrosialin: 5′ CAAG-GTCCAGGGAGG TTGTG 3′ (forward), 5′ CCAAAG-GTAAGCTGTCCATAAGGA 3′ (reverse), 5′ CGGTACC-CATCCCCACCTGTCTCTCTC 3′ (probe); CD36: 5′ TCCAGCCAATGCCTTTGC 3′ (forward), 5′ TGGAGAT-TACTTTTCAGTGCAGAA 3′ (reverse), 5′ TCACCCCTCCA-GAATCCAGACAACCA 3′ (probe); SR-A: 5′ CATGAACGA-GAGGATGCTGACT 3′ (forward), 5′ GGAAGGGATGCTGTCATTGAA 3′ (reverse), 5′ CAGTTCAGAATCCGTGAAATTTGACGCAC 3′ (probe); and GAPDH: 5′ CCACCCATGGCAAATTCC 3′ (forward), 5′ TGGGATTTCCATTGATGACAAG 3′ (reverse), 5′ TGGCACCGTCAAGGCTGAGAACG 3′ (probe). Equal amounts of cDNA were used in triplicate and amplified with the Taqman Master Mix provided by Perkin-Elmer. Amplification efficiencies were validated and normalized against GAPDH and nanograms of product were calculated using the standard curve method for quantitation against cDNA that was reverse transcribed from isolated aortas of LDLR$^{-/-}$ mice fed a 1.25% cholesterol and 21% milk-fat diet for 4 months. Total RNA that was not reverse transcribed was also analyzed to determine genomic DNA contamination.

Statistical analysis. Groups were compared by ANOVA and unpaired t tests using the StatView analysis program (SAS Institute Inc., Cay, North Carolina, USA). Data are expressed as the mean plus or minus SEM.

Results

Intervention studies were performed in LDLR$^{-/-}$ mice fed a Western-style diet for 10 weeks, starting at age 8–12 weeks. To reduce the possibility that effects of a single PPARγ ligand on atherosclerosis resulted from PPARγ-independent mechanisms, two distinct PPARγ agonists were used: rosiglitazone and GW7845. Rosiglitazone is a member of the TDZ class of insulin sensitizers that was developed using rodent models of type 2 diabetes. It has an effective concentration of 50% (EC$_{50}$) for murine PPARγ of 76 nM (33). GW7845 is a member of the tyrosine-based class of insulin sensitizers that was developed using human PPARγ as a molecular target. It has an EC$_{50}$ for murine PPARγ of 1.2 nM (33). Both drugs are highly specific for PPARγ, with EC$_{50}$ for PPARα and PPARδ in excess of 10 μM (33). We initially performed a pilot study using a calculated dose of 20 mg rosiglitazone/kg/day to establish appropriate dietary cholesterol content and extent of atherosclerosis. Rosiglitazone exerted a significant antiatherogenic effect in male mice in this study, but not in female mice (data not shown). However, because the 1.25% added dietary cholesterol resulted in serum cholesterol levels in excess of 2,000 mg/dL, a potential protective effect in females could have been overwhelmed. Two subsequent intervention studies were therefore carried out in which the added cholesterol was reduced to 0.01%. Each experiment resulted in the same pattern of responses to dietary and drug treatments, and the data from the two studies were pooled to increase statistical power.

Table 1
Average weights, cholesterol, triglyceride, and HDL$_c$ levels

	Weight g	Total Cholesterol mg/dL	Triglycerides mg/dL	HDL$_c$ mg/dL		Weight g	Total Cholesterol mg/dL	Triglycerides mg/dL	HDL$_c$ mg/dL
Males Control (*n* = 10)					**Females** Control (*n* = 10)				
T = 0 weeks	24.4 ± 0.8	258 ± 11	128 ± 17		T = 0 weeks	19.0 ± 0.7	235 ± 12	37 ± 12	
T = 4 weeks	36.7 ± 1.2	1258 ± 143	1150 ± 195		T = 4 weeks	24.1 ± 1.9	1053 ± 97	576 ± 258	
T = 8 weeks	38.9 ± 1.3	1552 ± 83	1279 ± 170		T = 8 weeks	27.2 ± 1.3	1211 ± 68	621 ± 207	
T = 10 weeks	42.5 ± 1.4	1549 ± 89	1226 ± 153	127 ± 5	T = 10 weeks	28.4 ± 1.7	1240 ± 109	722 ± 241	115 ± 4
Ro (*n* = 12)					**Ro** (*n* = 10)				
T = 0 weeks	26.1 ± 0.9	245 ± 10	121 ± 20		T = 0 weeks	20.4 ± 0.5	242 ± 6	47 ± 11	
T = 4 weeks	36.7 ± 1.3	1258 ± 103	1150 ± 265		T = 4 weeks	23.7 ± 1.1	1027 ± 6	624 ± 24	
T = 8 weeks	38.6 ± 1.4	1371 ± 72	1366 ± 134		T = 8 weeks	27.6 ± 1.1	1395 ± 81	1000 ± 107	
T = 10 weeks	40.4 ± 1.3	1440 ± 69	1541 ± 126	115 ± 4[A]	T = 10 weeks	29.7 ± 1.3	1513 ± 55[A]	1251 ± 69[B]	96 ± 3[B]
GW7845 (*n* = 10)					**GW7845** (*n* = 7)				
T = 0 weeks	26.3 ± 0.9	249 ± 9	116 ± 22		T = 0 weeks	20.0 ± 0.8	232 ± 11	48 ± 12	
T = 4 weeks	33.5 ± 3.5	1275 ± 168	1406 ± 276		T = 4 weeks	25.0 ± 1.1	1139 ± 82	927 ± 145	
T = 8 weeks	39.9 ± 1.0	1533 ± 81	1790 ± 184		T = 8 weeks	28.6 ± 1.2	1395 ± 90	1049 ± 131	
T = 10 weeks	41.7 ± 2.2	1626 ± 109	1507 ± 200	123 ± 3	T = 10 weeks	28.5 ± 1.4	1449 ± 136	1228 ± 157[B]	104 ± 4[A]

Data are expressed as the mean ± SEM; *n* represents the number of mice per group. Values were determined in plasma samples from nonfasting animals. Ro, rosiglitazone. [A]*P* < 0.05 and [B]*P* < 0.005, drug treatment group vs. control group.

At a dose of 20 mg/kg/day, rosiglitazone plasma levels averaged 6.4 plus or minus 0.06 μg/mL in male mice and 5.1 plus or minus 0.69 μg/mL in female mice at 10 weeks. GW7845 levels averaged 3.2 plus or minus 0.39 μg/mL in male mice and 3.2 plus or minus 0.46 μg/mL in female mice after 10 weeks of treatment. These serum levels are sufficient to exert inhibitory effects on proinflammatory gene expression in vitro (29). All animals appeared healthy throughout the study. Serum aspartate aminotransferase and alkaline phosphatase levels were used to assess potential liver toxicity and were not altered at the end of the study (data not shown). Histologic analysis of the bone marrow indicated a significant increase in percentage of marrow fat, and marked extramedullary hematopoiesis was observed in both male and female mice (data not shown). There were no significant changes in complete blood counts or hemoglobin. Data for body weight, total cholesterol, triglycerides, and HDL$_c$ at specific time points are presented in Table 1. The body weights in all groups increased during the intervention period, but the relative weight gain in males was greater than that in females. The Western diet resulted in a marked increase in total cholesterol within 1 month; the total cholesterol then remained constant at approximately 1,500 mg/dL in males. There was a slight increase in

Table 2
Average glucose, insulin, HbA$_{1c}$, NEFA levels

	Glucose mg/dL	Insulin ng/mL	Hb A$_{1c}$ %	NEFA mEq/L		Glucose mg/dL	Insulin ng/mL	Hb A$_{1c}$ %	NEFA mEq/L
Males Control (*n* = 10)					**Females** Control (*n* = 10)				
T = 0 weeks	307 ± 20	1.12 ± 0.17	5.50 ± 0.16		T = 0 weeks	267 ± 11	0.55 ± 0.04	5.57 ± 0.15	
T = 4 weeks	211 ± 24	1.38 ± 0.25	5.62 ± 0.11		T = 4 weeks	299 ± 14	1.48 ± 0.18	5.39 ± 0.05	
T = 8 weeks	245 ± 14	4.18 ± 0.41	5.29 ± 0.07		T = 8 weeks	273 ± 21	1.95 ± 0.49	4.96 ± 0.10	
T = 10 weeks	344 ± 22	4.24 ± 0.30	5.31 ± 0.13	0.60 ± 0.06	T = 10 weeks	347 ± 16	1.44 ± 0.30	5.11 ± 0.16	0.64 ± 0.06
Ro (*n* = 12)					**Ro** (*n* = 10)				
T = 0 weeks	282 ± 13	0.95 ± 0.08	5.46 ± 0.11		T = 0 weeks	250 ± 8	0.63 ± 0.13	5.39 ± 0.15	
T = 4 weeks	211 ± 11	1.38 ± 0.11	5.62 ± 0.11		T = 4 weeks	210 ± 10	0.75 ± 0.05	5.78 ± 0.03	
T = 8 weeks	207 ± 8	2.03 ± 0.44	5.08 ± 0.13		T = 8 weeks	216 ± 10	1.91 ± 0.53	4.94 ± 0.09	
T = 10 weeks	315 ± 10	1.45 ± 0.33[B]	4.91 ± 0.12[A]	0.65 ± 0.04	T = 10 weeks	312 ± 11	0.93 ± 0.33	4.87 ± 0.07	0.85 ± 0.11
GW7845 (*n* = 10)					**GW7845** (*n* = 7)				
T = 0 weeks	317 ± 8	1.01 ± 0.18	5.78 ± 0.06		T = 0 weeks	261 ± 14	0.94 ± 0.13	5.20 ± 0.16	
T = 4 weeks	211 ± 13	1.54 ± 0.49	5.76 ± 0.11		T = 4 weeks	225 ± 16	1.07 ± 0.15	5.47 ± 0.12	
T = 8 weeks	204 ± 14	2.01 ± 0.32	5.32 ± 0.09		T = 8 weeks	190 ± 6	1.75 ± 0.59	4.75 ± 0.07	
T = 10 weeks	311 ± 13	1.65 ± 0.36[B]	4.81 ± 0.16[A]	0.63 ± 0.05	T = 10 weeks	311 ± 13	1.29 ± 0.37	4.80 ± 0.16	0.81 ± 0.08

Data are expressed as the mean ± SEM; *n* represents the number of mice per group. Values were determined in plasma samples from nonfasting animals. Ro, rosiglitazone. [A]*P* < 0.05 and [B]*P* < 0.005, drug treatment group vs. control group.

cholesterol levels of treated females, but this effect only reached statistical significance ($P = 0.05$) in the rosiglitazone treatment group after 10 weeks. Triglycerides were significantly increased and HDL_c levels were decreased in female mice treated with rosiglitazone or GW7845. A decrease in HDL_c levels was seen in male mice treated with rosiglitazone only.

PPARγ ligands inhibit the development of atherosclerosis in male mice. Atherosclerosis at the aortic origin was determined by computer-assisted image analysis as described previously (32). Male and female control animals exhibited similar levels of atherosclerosis. Lesions were observed underneath most of the valve leaflets, with some lesions exhibiting areas of central necrosis (Figure 1a). Macroscopically detectable lesions were generally absent from the thoracic or abdominal aorta (data not shown). Markedly fewer and smaller lesions were found in male mice that were treated with either rosiglitazone or GW7845, with quantitative analysis indicating a 60 to 80% reduction in lesion area (Figure 1b). In contrast, the extent of atherosclerosis in female mice treated with either rosiglitazone or GW7845 was not statistically different from that in control mice, confirming the findings of the initial pilot study.

Metabolic effects of PPARγ ligands. To investigate possible mechanisms accounting for antiatherogenic effects of PPARγ ligands in male mice and lack of these effects in female mice, lipoprotein levels were evaluated in control and treatment groups. Fast-performance liquid chromatography (FPLC) analysis of pooled terminal serum samples indicated that GW7845 and rosiglitazone had no effect on the lipoprotein profile in male mice (Figure 2a). In contrast, in female mice the VLDL, IDL, and LDL fractions were increased and the HDL fraction decreased in both the rosiglitazone and GW7845 treatment groups (Figure 2b).

Effects of PPARγ ligands on serum glucose, insulin, HbA_{1c}, and NEFA levels are presented in Table 2. The Western diet itself did not significantly alter glucose, HbA_{1c}, or NEFA levels, but insulin levels rose in both male and female mice. Rosiglitazone and GW7845 treatment resulted in a significant decrease in insulin levels in male mice but had no significant effect on insulin levels in female mice (Table 2). HbA_{1c} decreased in males treated with rosiglitazone and GW7845.

To further investigate the effects of rosiglitazone and GW7845 on glucose homeostasis, the response to an oral glucose challenge was assessed in LDLR$^{-/-}$ mice fed the Western diet for 8 weeks. LDLR$^{-/-}$ mice fed a normal chow diet were used as additional control groups. Mice were fasted for 4 hours before being given an oral glucose load of 0.75 mg/g. Blood samples were taken at 0, 15, 30, 60, and 90 minutes for measurement of glucose and insulin levels. In male mice, the Western diet had relatively little effect on glucose levels in response to the oral glucose challenge (Figure 3a). In female mice, after glucose administration, the Western diet resulted in modest elevations in glucose that were normalized by treatment with either rosiglitazone or GW7845 (Figure 3b). Striking differences in the insulin responses to oral glucose challenge were noted between
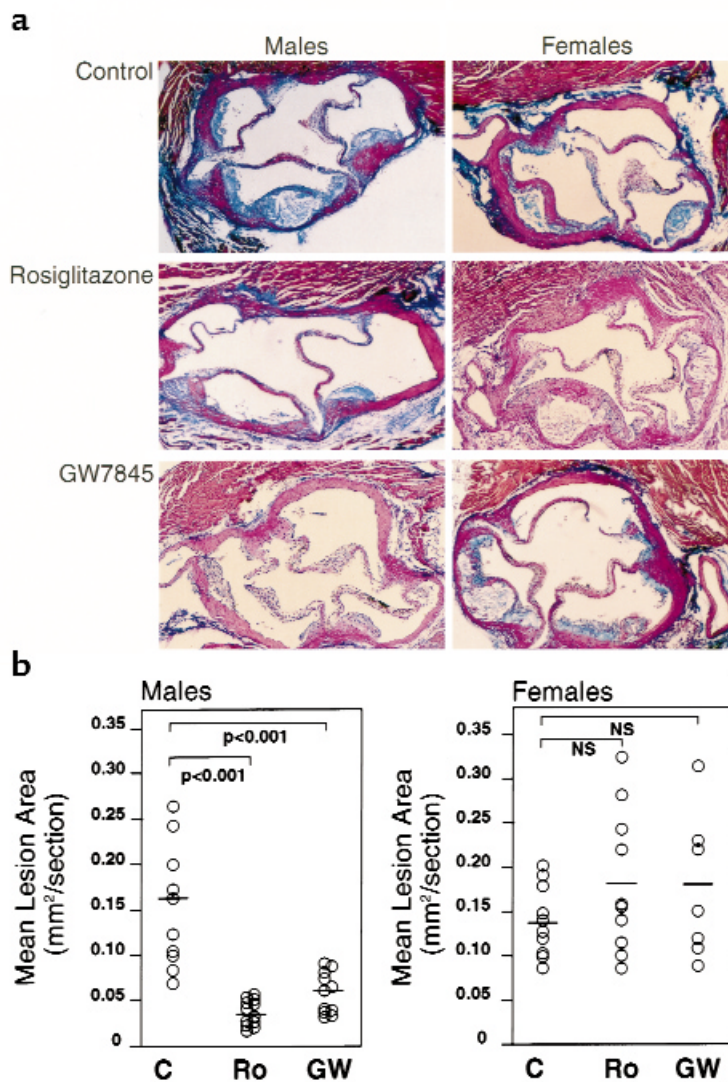

Figure 1

Atherosclerosis in LDLR$^{-/-}$ mice fed a high-fat, cholesterol-enriched Western diet for 10 weeks. (**a**) Sections through the aortic root at the levels of the aortic valves were stained for elastin to highlight the medial boundaries of atherosclerotic lesions. (**b**) Quantitative analysis of lesion areas in control mice (C), mice treated with rosiglitazone (Ro), and mice treated with GW7845 (GW). For male mice, means ± SEM were: C, 0.161 ± 0.067 mm^2/section ($n = 10$); Ro, 0.037 ± 0.014 mm^2/section ($n = 12$); GW, 0.063 ± 0.027 mm^2/section ($n = 10$). For female mice, means ± SEM were: C, 0.131 ± 0.035 mm^2/section ($n = 10$); Ro, 0.183 ± 0.0.088 mm^2/section ($n = 10$); GW, 0.181±0.0091 mm^2/section ($n = 10$). NS, not statistically significant.

male and female mice treated with rosiglitazone and GW7845. The Western diet resulted in increased fasting insulin levels in both male and female mice (Figure 3, c and d), compared with the chow-fed controls. Treatment with rosiglitazone or GW7845 resulted in normalization of the fasting insulin levels and the insulin response to glucose challenge in male mice, but not in female mice (Figure 3, c and d), consistent with changes in insulin levels observed in the intervention studies (Table 2).

Effects of PPARγ ligands on gene expression. To investigate potential effects of PPARγ ligands on patterns of gene expression within the arterial wall, RNA analysis was performed in LDLR$^{-/-}$ mice fed a Western diet for 10 weeks in the absence or presence of rosiglitazone or GW7845 as described for the intervention studies. RNA was isolated from the base of the heart containing the aortic origin affected by atherosclerosis and analyzed for TNF-α, MCP-1, VCAM-1, and gelatinase B mRNA levels, using quantitative real-time PCR. TNF-α and

gelatinase B mRNA levels were significantly lower in male mice treated with rosiglitazone or GW7845 (Figure 4). Decreases in TNF-α and gelatinase B were smaller in female mice and did not reach statistical significance in the case of gelatinase B. Levels of VCAM-1 and MCP-1, which are thought to be involved in monocyte adhesion to the vessel wall and migration into the lesion, respectively (34), did not change significantly among the groups (Figure 4). Reductions in TNF-α and gelatinase B mRNA levels were also observed in RNA prepared from the apex of the heart, suggesting general effects of the PPARγ ligands (data not shown). Differences in the responses of TNF-α and gelatinase B genes to PPARγ ligand between male and female mice were not likely due to differences in PPARγ expression, because PPARγ mRNA levels were approximately two times higher in female tissues (data not shown).

Because there were significant differences in lesion size in male controls and animals treated with solvent, rosiglitazone, or GW7845, we also investigated whether PPARγ ligands altered levels of gene expression in the artery wall under conditions of equivalent degrees of atherosclerosis. LDLR$^{-/-}$ male mice were fed a 1.25% cholesterol and 21% milk-fat diet for 16 weeks to induce significant atherosclerosis in the aortic arch. Mice were then treated with rosiglitazone, GW7845, or control solvent for 2 weeks while maintaining the high-fat, high-cholesterol diet. Aortas were dissected and weighed to confirm comparable levels of atherosclerosis (35). As an additional control group, mRNA was isolated from aortas of normocholesterolemic animals. The aortas from each group were pooled, and mRNA was isolated for analysis of macrosialin, CD36, SR-A, MCP-1, TNF-α, and VCAM-1 gene expression (Figure 5). Macrosialin is a macrophage-specific membrane glycoprotein that serves as a marker of tissue macrophages (36). Macrosialin expression was low in normal aortas and markedly increased in atherosclerotic aortas, as expected. Macrosialin levels were not significantly altered by 2 weeks of treatment with rosiglitazone or GW7845, consistent with our observation that PPARγ ligands do not alter macrosialin expression in peritoneal macrophages (data not shown) and reflecting comparable levels of atherosclerosis in these three groups. SR-A and MCP-1 mRNA levels were also elevated in atherosclerotic aortas, as expected. Surprisingly, the mRNA levels for VCAM-1 remained unchanged. In contrast to previous findings in cell-culture models (29, 37), mRNA levels for these genes were not decreased by treatment with PPARγ ligands. However, treatment with rosiglitazone or GW7845 significantly increased CD36 expression and inhibited TNF-α expression, indicating actions of PPARγ on gene expression in the artery wall. The effects on CD36 expression were tissue specific, because no increase in CD36 expression was observed in cardiac tissue of mice treated with rosiglitazone or GW7845 (data not shown).
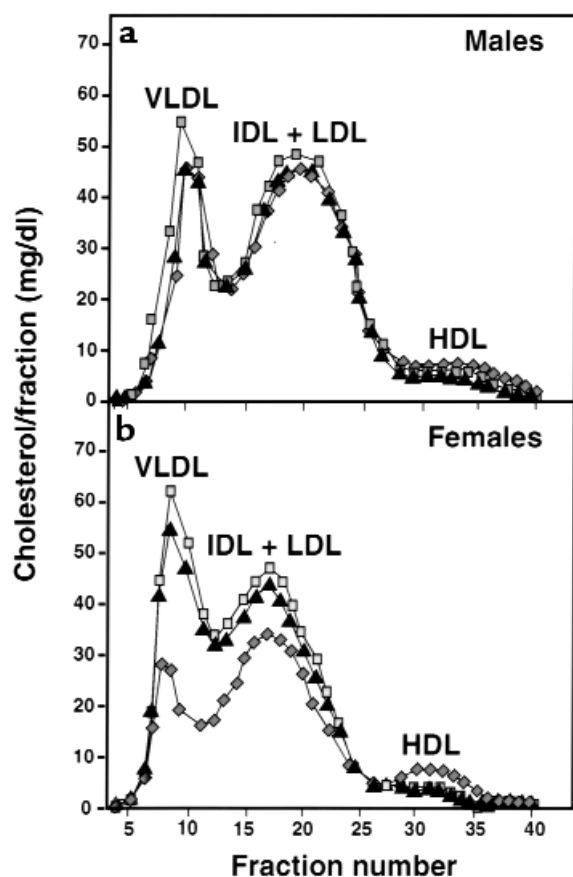

Figure 2
Size distribution of lipoprotein particles in LDLR$^{-/-}$ mice fed a high-fat, cholesterol-enriched diet and treated with solvent (control; diamonds), rosiglitazone (squares), or GW7845 (triangles) for 10 weeks. Plasma was pooled from four mice from each treatment group and fractionated by FPLC. Mean cholesterol content in each fraction was determined in duplicate.

Figure 3

Glucose and insulin responses to an oral glucose challenge in LDLR$^{-/-}$ mice fed the normal chow (circles); high-fat, cholesterol-enriched diet and solvent (control; diamonds); rosiglitazone (squares); or GW7845 (triangles). Blood glucose and plasma insulin levels were determined at base line (after a 4-hour fast) and 15, 30, 60, and 90 minutes after oral administration of 0.75 mg glucose/g body weight. Samples were taken from eight animals per group. Data are expressed as the mean ± SEM. ^{A}P < 0.0001, ^{B}P < 0.002, ^{C}P < 0.015, and ^{D}P < 0.04, drug treatment group vs. control group.
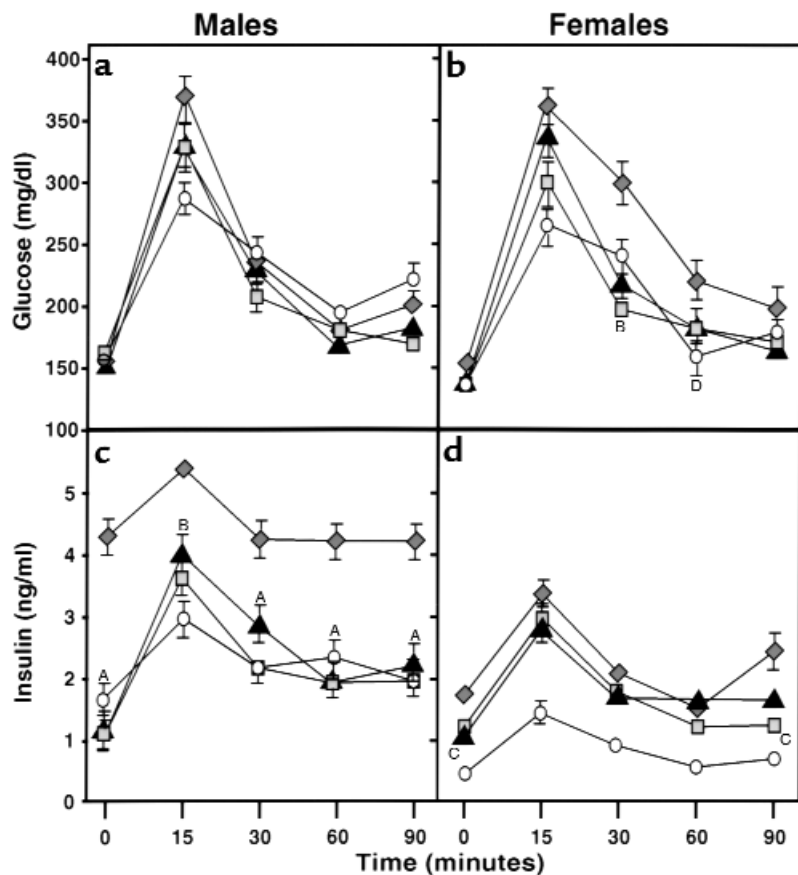
Discussion

The present studies demonstrate that PPARγ ligands significantly inhibit the development of atherosclerosis in LDLR$^{-/-}$ male mice fed a Western-style diet. These mice, in addition to being hypercholesterolemic, were obese, hypertriglyceridemic, and insulin resistant. They thus exhibit clinical features of many human diabetic patients who are candidates for treatment with PPARγ ligands. Rosiglitazone and GW7845 reduced the extent of atherosclerosis despite a significant increase in the expression of CD36 in the vessel wall. These observations suggest that the potential of PPARγ ligands to promote the development of foam cells by upregulation of CD36 is overcome by other systemic and local actions. Several mechanisms could potentially account for the net antiatherosclerotic effects of rosiglitazone and GW7845. A number of proinflammatory cytokines, including TNF-α, IL-1α, and IL-1β, have been suggested to promote the development of atherosclerosis (38). Systemic reductions in the circulating levels of these cytokines or reductions in their expression within cells of the artery wall could potentially underlie at least some of the antiatherosclerotic effects of rosiglitazone and GW7845. Although previous studies have suggested effects of PPARγ ligands on MCP-1 expression in macrophages and smooth muscle cells and VCAM-1 expression in endothelial cells (18, 39–41), we did not observe significant alter-ations in VCAM-1 or MCP-1 expression in mice treated with PPARγ agonists. This may reflect the cellular heterogeneity of the aortic origin and vessel wall from which RNA was isolated for analysis. The antiatherogenic effects of rosiglitazone and GW7845 in male mice also correlated with improved insulin sensitivity. However, to date, no experimental evidence for a direct influence of insulin resistance on atherosclerosis has been provided in humans or murine models (42). Further investigation will be required to establish the major mechanisms underlying the therapeutic effects of PPARγ ligands in this model system.
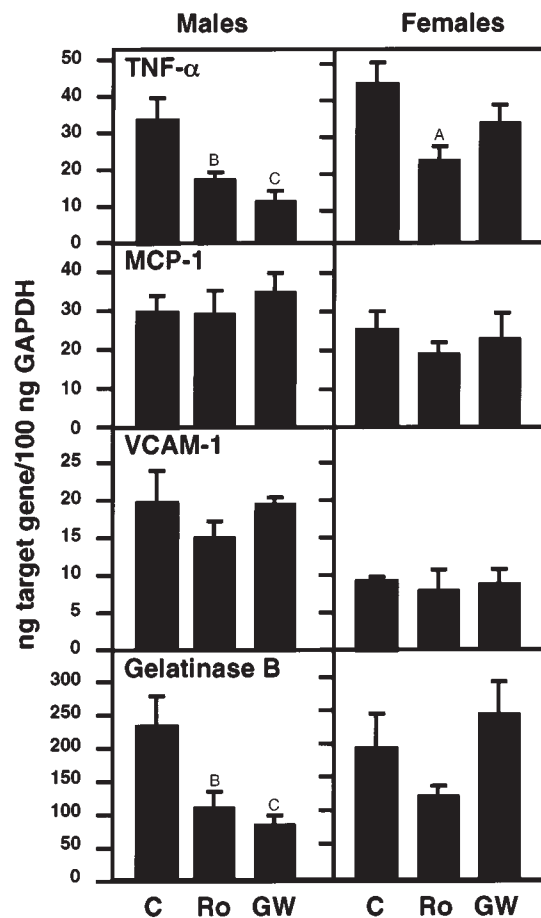
Intriguingly, female mice did not exhibit a reduction in atherosclerosis in response to PPARγ-specific ligands. This lack of a response was not due to altered drug levels or differences in levels of PPARγ expression in the artery wall. Rosiglitazone and GW7845 were less effective in correcting hyperinsulinemia in female mice and did not influence the expression of gelatinase B or TNF-α in tissues. In contrast to male mice, PPARγ ligands altered the lipoprotein size distribution in female mice, reducing HDL levels and skewing the profile to larger particles. Reductions in HDL levels could potentially account for lack of effect of rosiglitazone and GW7845 on the extent of atherosclerosis, but the lack of effect on gelatinase B and TNF-α levels suggest gender-specific differences in the responses to

Figure 4

Expression of TNF-α, MCP-1, VCAM-1, and gelatinase B mRNA in the aortic root. The mRNA levels were quantitated using real-time RT-PCR. Six to seven samples per group were analyzed. C, control; Ro, rosiglitazone; GW, GW7845. Data are expressed as mean ± SEM. $^{A}P < 0.05$, $^{B}P < 0.01$, and $^{C}P < 0.001$, drug treatment groups vs. cholesterol group.

PPARγ ligands. The basis for these differences is unclear, but they are likely to relate to influences of estrogens and progestins. Consistent with this, preliminary studies of ovariectomized female mice indicate metabolic responses to rosiglitazone and GW7845 that are much more similar to male mice. Studies of the efficacy of TZDs as insulin sensitizers in human diabetic patients have not revealed any significant gender-specific differences, but most female patients enrolled in these studies are postmenopausal.

In concert, these studies provide clear evidence that activation of PPARγ inhibits the development of atherosclerosis in a murine model. These effects were observed using relatively high doses of PPARγ ligands that also induced adipogenesis in bone marrow and secondary extramedullary hematopoiesis. Extending this proof of principle to human populations will require clinical investigation in diabetic and nondiabetic patients. Because the PPARγ agonists used in these studies exerted both potentially antiatherogenic (e.g., downregulation of TNF-α) and potentially proatherogenic (e.g., upregulation of CD36) effects on patterns of gene expression in the artery wall, the development of novel PPARγ ligands that dissociate proatherogenic activities from antidiabetic and antiatherogenic activities would be highly desirable. Recent successes in the development of selective estrogen receptor modulators (43) suggest that such goals are attainable.

Figure 5

Expression of macrosialin, CD36, SR-A, MCP-1, TNF-α, and VCAM-1 mRNA in the aorta. Male LDLR$^{-/-}$ mice were fed either a normal chow diet (N) or a high-cholesterol diet for 4 months to induce the development of atherosclerosis (Athero). Animals fed the high-cholesterol diet were then treated with either solvent control, rosiglitazone, or GW8745 for 2 weeks. The mRNA levels were quantitated using real-time RT-PCR. Data represent pooled aortas with an average weight of 3.86 ± 0.16 mg/aorta for normal chow (N) (n = 11); 5.75 ± 0.67 mg/aorta for high cholesterol (C)(n = 6); 5.67 ± 0.56 mg/aorta for high cholesterol/rosiglitazone (Ro) (n = 6); and 5.80 ± 0.70 mg/aorta for high cholesterol/GW7845 (GW) (n = 6). Data are in triplicates and expressed as mean ± SEM.
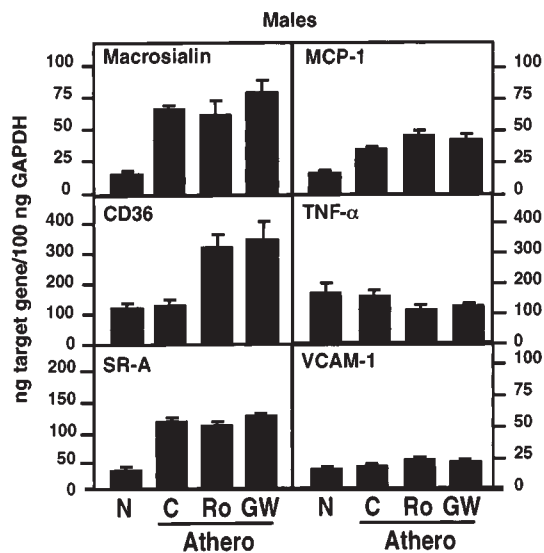
1. Kannel, W., and McGee, D. 1979. Diabetes and cardiovascular disease: the Framingham study. *JAMA.* **241**:2035–2038.
2. Uusitupa, M., Niskanen, L., and Siitonen, O. 1990. 5-year incidence of atherosclerotic vascular disease in relation to general risk factors, insulin levels, and abnormalities in lipoprotein composition in non-insulin-dependent diabetic and nondiabetic subjects. *Circulation.* **82**:27–36.
3. Steinberg, D., Parthasarathy, S., Carew, T.E., Khoo, J.C., and Witztum, J.L. 1989. Beyond cholesterol. Modifications of low-density lipoprotein that increase its atherogenicity. *N. Engl. J. Med.* **320**:915–924.
4. Napoli, C., et al. 1997. Fatty streak formation occurs in human fetal aortas and is greatly enhanced by maternal hypercholesterolemia. Intimal accumulation of low density lipoprotein and its oxidation precede monocyte recruitment into early atherosclerotic lesions. *J. Clin. Invest.* **100**:2680–2690.
5. Kodama, T., Reddy, P., Kishimoto, C., and Krieger, M. 1988. Purification and characterization of a bovine acetyl low density lipoprotein receptor. *Proc. Natl. Acad. Sci. USA.* **85**:9238–9242.
6. Endemann, G., et al. 1993. CD36 is a receptor for oxidized low density lipoprotein. *J. Biol. Chem.* **268**:11811–11816.
7. Ramprasad, M.P., Terpstra, V., Kondratenko, N., Quehenberger, O., and Steinberg, D. 1996. Cell surface expression of mouse macrosialin and human CD68 and their role as macrophage receptors for oxidized low density lipoprotein. *Proc. Natl. Acad. Sci. USA.* **93**:14833–14838.
8. Ross, R. 1986. The pathogenesis of atherosclerosis. *N. Engl. J. Med.* **314**:488–500.
9. Ross, R. 1999. Atherosclerosis: an inflammatory disease. *N. Engl. J. Med.* **340**:115–126.
10. Boring, L., Gosling, J., Cleary, M., and Charo, I.F. 1998. Decreased lesion formation in CCR2–/– mice reveals a role for chemokines in the initiation of atherosclerosis. *Nature.* **394**:894–897.
11. Gosling, J., et al. 1999. MCP-1 deficiency reduces susceptibility to atherosclerosis in mice that overexpress human apolipoprotein B. *J. Clin. Invest.* **103**:773–778.
12. Suzuki, H., et al. 1997. A role for macrophage scavenger receptors in atherosclerosis and susceptibility to infection. *Nature.* **386**:292–296.
13. Febraio, M., et al. 2000. Targeted disruption of the class B scavenger receptor CD36 protects against atherosclerotic lesion development in mice. *J. Clin. Invest.* **105**:1049–1056.
14. Barnes, P.J., and Karin, M. 1997. Nuclear factor-kappaB: a pivotal transcription factor in chronic inflammatory diseases. *N. Engl. J. Med.* **336**:1066–1071.
15. Sato, H., Kita, M., and Seiki, M. 1993. v-Src activates the expression of 92-kDa type IV collagenase gene through the AP-1 site and the GT box homologous to retinoblastoma control elements. A mechanism regulating gene expression independent of that by inflammatory cytokines. *J. Biol. Chem.* **268**:23460–23468.
16. Ricote, M., et al. 1998. Expression of the peroxisome proliferator-activated receptor γ (PPARγ) in human atherosclerosis and regulation in macrophages by colony stimulating factors and oxidized low density lipoprotein. *Proc. Natl. Acad. Sci. USA.* **95**:7614–7619.
17. Marx, N., Sukhova, G., Murphy, C., Libby, P., and Plutzky, J. 1998. Macrophages in human atheroma contain PPARgamma: differentiation-dependent peroxisomal proliferated-activated receptor gamma expression and reduction of MMP-9 activity through PPARgamma activation in mononuclear phagocytes *in vitro. Am. J. Pathol.* **153**:17–23.
18. Jackson, S.M., et al. 1999. Peroxisome proliferator-activated receptor activators target human endothelial cells to inhibit leukocyte-endothelial cell interaction. *Arterioscler. Thromb. Vasc. Biol.* **19**:2094–2104.
19. Tontonoz, P., Nagy, L., Alvarez, J.G.A., Thomazy, V.A., and Evans, R.M. 1998. PPARγ promotes monocyte/macrophage differentiation and uptake of oxidized LDL. *Cell.* **93**:241–252.
20. Pasceri, V., Wu, H.D., Willerson, J.T., and Yeh, E.T. 2000. Modulation of vascular inflammation in vitro and in vivo by peroxisome proliferator-activated receptor-gamma activators. *Circulation.* **101**:235–238.
21. Nagy, L., Tontonoz, P., Alvarez, J.G.A., Chen, H., and Evans, R.M. 1998. Oxidized LDL regulates macrophage gene expression through ligand activation of PPAR-gamma. *Cell.* **93**:229–240.
22. Forman, B.M., et al. 1995. 15-Deoxy-$\Delta^{12,14}$-prostaglandin J$_2$ is a ligand for the adipocyte determination factor PPARγ. *Cell.* **83**:803–812.
23. Kliewer, S.A., et al. 1997. Fatty acids and eicosanoids regulate gene expression through direct interactions with peroxisome proliferator-activated receptors α and γ. *Proc. Natl. Acad. Sci. USA.* **94**:4318–4323.
24. Barak, Y., et al. 1999. PPARγ is required for placental, cardiac, and adipose tissue development. *Mol. Cell.* **4**:585–595.
25. Kubota, N., et al. 1999. PPARγ mediates high-fat diet-induced adipocyte hypertrophy and insulin resistance. *Mol. Cell.* **4**:597–609.
26. Rosen, E.D., et al. 1999. PPARγ is required for the differentiation of adipose tissue in vivo and in vitro. *Mol. Cell.* **4**:611–617.
27. Nolan, J.J., Ludvik, B., Beerdsen, P., Joyce, M., and Olefsky, J. 1994. Improvement in glucose tolerance and insulin resistance in obese subjects treated with troglitazone. *N. Engl. J. Med.* **331**:1188–1193.
28. Jiang, C., Ting, A.T., and Seed, B. 1998. PPAR-gamma agonists inhibit production of monocyte inflammatory cytokines. *Nature.* **391**:82–86.
29. Ricote, M., Li, A.C., Willson, T.M., Kelly, C.J., and Glass, C.K. 1998. The peroxisome proliferator-activated receptor-γ is a negative regulator of macrophage activation. *Nature.* **391**:79–82.
30. Su, C.G., et al. 1999. A novel therapy for colitis utilizing PPAR-γ ligands to inhibit the epithelial inflammatory response. *J. Clin. Invest.* **104**:383–389.
31. Sheehan, D.C., and Hrapchak, B.B. 1980. *Theory and practice of histotechnology.* C.V. Mosby Co., St. Louis, Missouri, USA. 481 pp.
32. Tangirala, R.K., Rubin, E.M., and Palinski, W. 1995. Quantitation of atherosclerosis in murine models: correlation between lesions in the aortic origin and in the entire aorta, and differences in the extent of lesions between sexes in LDL receptor-deficient and apoprotein E-deficient mice. *J. Lipid Res.* **36**:1–9.
33. Willson, T., Brown, P., Sternbach, D., and Henke, B. 2000. The PPARs: from orphan receptors to drug discovery. *J. Med. Chem.* **43**:527–550.
34. Fruebis, J., Gonzales, V., Silvestre, M., and Palinski, W. 1997. Effect of probucol treatment on gene expression of VCAM-1, MCP-1 and M-CSF in the aortic wall of LDL receptor-deficient rabbits during early atherogenesis. *Arterioscler. Thromb. Vasc. Biol.* **17**:1289–1302.
35. Tsimikas, S., Shortal, B.P., Witztum, J.L., and Palinski, W. 2000. In vivo uptake of radiolabeled MDA2, an oxidation-specific monoclonal antibody, provides an accurate measure of atherosclerotic lesions rich in oxidized LDL and is highly sensitive to their regression. *Arterioscler. Thromb. Vasc. Biol.* **20**:689–697.
36. Holness, C.L., and Simmons, D.L. 1993. Molecular cloning of CD68, a human macrophage marker related to lysosomal glycoproteins. *Blood.* **81**:1607–1613.
37. Goetze, S., et al. 1999. PPAR gamma-ligands inhibit migration mediated by multiple chemoattractants in vascular smooth muscle cells. *J. Cardiovasc. Pharmacol.* **33**:798–806.
38. Libby, P., Sukhova, G., Lee, R.T., and Galis, Z.S. 1995. Cytokines regulate vascular functions related to stability of the atherosclerotic plaque. *J. Cardiovasc. Pharmacol.* **25**(Suppl. 2):S9–S12.
39. Murao, K., et al. 1999. Thiazolidinedione inhibits the production of monocyte chemoattractant protein-1 in cytokine-treated human vascular endothelial cells. *FEBS Lett.* **454**:27–30.
40. Law, R.E., et al. 1996. Troglitazone inhibits vascular smooth muscle cell growth and intimal hyperplasia. *J. Clin. Invest.* **98**:1897–1905.
41. Staels, B., et al. 1998. Activation of human aortic smooth-muscle cells is inhibited by PPARalpha but not by PPARgamma activators. *Nature.* **393**:790–793.
42. Merat, S., Casanada, F., Sutphin, M., Palinski, W., and Reaven, P.D. 1999. Western-type diets induce insulin resistance and hyperinsulinemia in LDL receptor-deficient mice but do not increase aortic atherosclerosis compared with normoinsulinemic mice in which similar plasma cholesterol levels are achieved by a fructose-rich diet. *Arterioscler. Thromb. Vasc. Biol.* **19**:1223–1230.
43. Roe, E.B., Chiu, K.M., and Arnaud, C.D. 2000. Selective estrogen receptor modulators and postmenopausal health. *Adv. Intern. Med.* **45**:257–278.